Quantitative role of LAL, NPC2, and NPC1 in lysosomal cholesterol processing defined by genetic and pharmacological manipulations

Charina M. Ramirez,[1,*] Benny Liu,[1,†] Amal Aqul,[*] Anna M. Taylor,[§] Joyce J. Repa,[†,§] Stephen D. Turley,[†] and John M. Dietschy[2,†]

Departments of Pediatrics,[*] Internal Medicine,[†] and Physiology,[§] University of Texas Southwestern Medical School, Dallas, TX 75390-9151

Abstract **Lipoprotein cholesterol taken up by cells is processed in the endosomal/lysosomal (E/L) compartment by the sequential action of lysosomal acid lipase (LAL), Niemann-Pick C2 (NPC2), and Niemann-Pick C1 (NPC1). Inactivation of NPC2 in mouse caused sequestration of unesterified cholesterol (UC) and expanded the whole animal sterol pool from 2,305 to 4,337 mg/kg. However, this pool increased to 5,408 and 9,480 mg/kg, respectively, when NPC1 or LAL function was absent. The transport defect in mutants lacking NPC2 or NPC1, but not in those lacking LAL, was reversed by cyclodextrin (CD), and the ED_{50} values for this reversal varied from ~40 mg/kg in kidney to >20,000 mg/kg in brain in both groups. This reversal occurred only with a CD that could interact with UC. Further, a CD that could interact with, but not solubilize, UC still overcame the transport defect. These studies showed that processing and export of sterol from the late E/L compartment was quantitatively different in mice lacking LAL, NPC2, or NPC1 function. In both *npc2*$^{-/-}$ and *npc1*$^{-/-}$ mice, the transport defect was reversed by a CD that interacted with UC, likely at the membrane/bulk-water interface, allowing sterol to move rapidly to the export site of the E/L compartment.**—Ramirez, C. M., B. Liu, A. Aqul, A. M. Taylor, J. J. Repa, S. D. Turley, and J. M. Dietschy. **Quantitative role of LAL, NPC2, and NPC1 in lysosomal cholesterol processing defined by genetic and pharmacological manipulations.** ***J. Lipid Res.*** **2011.** 52: **688–698.**

Supplementary key words Niemann-Pick type C disease • Wolman disease • liver disease • neurodegeneration • macrophage • inflammation • cholesterol balance • lysosomal acid lipase

Nearly all cells in the body, including neurons of the central nervous system (CNS), take up cholesteryl ester (CE) and/or unesterified cholesterol (UC) carried in various lipoproteins from the surrounding pericellular fluid by receptor-mediated and bulk-phase endocytosis (1, 2). The sterol in these particles is processed in the late endosomal/lysosomal (E/L) compartment of cells by the sequential action of at least three proteins, lysosomal acid lipase (LAL) (3), Niemann-Pick C2 (NPC2) (4), and Niemann-Pick C1 (NPC1) (5), before being exported into the cytosolic compartment. There it joins other UC, newly synthesized from acetyl-CoA, to provide a metabolically active pool of sterol critical for normal turnover of plasma membrane cholesterol. Because UC is a hydrophobic amphipath and potentially toxic to cells, the size of this metabolically active pool is tightly monitored by two systems, the sterol regulatory element binding proteins (SREBPs) (6) and the liver X receptors (LXRs) (7), which, in turn, regulate the expression of genes controlling the uptake, synthesis, degradation, and export of UC. In this manner, the size of the metabolically active pool is kept relatively small and constant even though rates of lipoprotein uptake and sterol synthesis may vary widely.

Mutations in any one of these three proteins cause accumulation of CE (LAL, Wolman disease) or UC (NPC2 or NPC1, Niemann-Pick C disease) in every tissue, which leads to cell dysfunction and death, and to a variety of clinical syndromes including disease of the liver, lungs, and

This work was supported by US Public Health Service grant R01 HL009610 (J.M.D. and S.D.T.), the Moss Heart Fund (J.M.D.), and the Ara Parseghian Medical Research Foundation (J.J.R.). The content is solely the responsibility of the authors and does not necessarily represent the official views of the National Heart, Lung, and Blood Institute or the National Institutes of Health. C.M.R. and B.L. also received post-doctoral support from the Ara Parseghian Medical Research Foundation and A.M.T. received predoctoral support from the Pharmacology Training Grant at UT Southwestern, NIH T32 GM007062-32.

Manuscript received 21 December 2010 and in revised form 31 Janaury 2011.

Published, JLR Papers in Press, February 2, 2011
DOI 10.1194/jlr.M013789

Abbreviations: ALT, alanine aminotransferase ; AST, aspartate aminotransferase ; bw, body weight; CD, cyclodextrin; CE, cholesteryl ester; CNS, central nervous system; E/L, endosomal/lysosomal; HP-α-CD, 2-hydroxypropyl-α-cyclodextrin; HP-β-CD, 2-hydroxypropyl-β-cyclodextrin; LAL, lysosomal acid lipase; LXR, liver X receptor; NPC2, Niemann-Pick C2; NPC1, Niemann-Pick C1; SBE7-β-CD, sulfobutyl ether-7-β-cyclodextrin; SREBP, sterol regulatory element binding protein; TC, total cholesterol; UC, unesterified cholesterol.

[1] C. M. Ramirez and B. Liu contributed equally to this work.
[2] To whom correspondence should be addressed.
Email: john.dietschy@utsouthwestern.edu

CNS. In an important recent observation, it was shown that acute administration of the cyclic oligosaccharide, 2-hydroxypropyl-β-cyclodextrin (HP-β-CD), to a murine model of NPC1 disease acutely overcame the block in export of UC from the late E/L compartment (8). The sudden flow of this sequestered UC into the metabolically active pool in the cytosol was inferred by a marked increase in the cytosolic level of CE, suppression of sterol synthesis, suppression of many SREBP-target genes and activation of several LXR-regulated genes. Furthermore, weekly administration of HP-β-CD to *npc1*$^{-/-}$ mice nearly normalized whole animal cholesterol pools, suppressed the inflammatory reaction characteristic of this disorder, prevented the liver disease, slowed the neurodegeneration, and prolonged life (9, 10). These findings raise the important issues of how HP-β-CD might interact with LAL, NPC2, or NPC1 and how it functions to bypass the intracellular transport defect seen in the NPC1 mouse.

It is known that certain cyclodextrins can solubilize UC and extract sterol from the plasma membrane of cells (11, 12). During this process, several cyclodextrin molecules must encompass the hydrophobic surfaces of the sterol molecule, thereby eliminating the ~28 kcal/mol of free energy necessary to pull the UC molecule into bulk-phase water (13). This is a slow process, requiring millimolar concentrations of cyclodextrin. However, recent observations have demonstrated that HP-β-CD reverses the export defect in the *npc1*$^{-/-}$ mouse very quickly, at micromolar concentrations, and under circumstances where no UC is found bound to the excreted cyclodextrin (14). These observations make it unlikely that solubilization of UC into the bulk-phase of the pericellular or E/L compartment fluid could account for the restoration of normal sterol transport seen in the *npc1*$^{-/-}$ mouse after cyclodextrin administration. Alternatively, some cyclodextrins can interact at a 1:1 molecular ratio with partially extruded UC molecules at a water/membrane interface, greatly accelerating the movement of the sterol along or between membranous structures. These interactions occur rapidly and at micromolar concentrations, do not involve solubilization of the UC molecule into the bulk-phase water, and are detected by changes in resonance frequency of UC-coated piezoelectric crystals or by alterations in surface pressure of UC monolayers (15, 16).

Taken together, these observations have highlighted a number of important areas concerning the intracellular processing and transport of UC where there are few quantitative data available. For example, whereas LAL, NPC2, and NPC1 are thought to be sequentially involved in the processing and export of UC through the late E/L compartment of all cells, there is currently no information on the magnitude of the defect in transport induced by inactivating mutations of each of these proteins. There are also few data on how compounds like the cyclodextrins might act within the E/L compartment to bypass the transport defect induced by mutations in any one of these three proteins. The present studies, therefore, were undertaken to use both genetic and pharmacological manipulations to explore these important questions. The first set of experiments quantitated in parallel groups of animals the magnitude of the transport defect when either LAL, NPC2, or NPC1 was inactivated. The second set of studies further explored these transport defects by comparing the ability of HP-β-CD to overcome the intracellular processing defect induced after inactivating each of these three proteins. The final set of experiments utilized a variety of structural variants of cyclodextrin to elucidate how these pharmacological agents may act within the late E/L compartment to overcome the defect in UC export.

MATERIAL AND METHODS

Animals

Control (*npc1*$^{+/+}$, *npc2*$^{+/+}$, and *lal*$^{+/+}$) and homozygous mutant (*npc1*$^{-/-}$, *npc2*$^{-/-}$, and *lal*$^{-/-}$) mice were generated from heterozygous (*npc1*$^{+/-}$, *npc2*$^{+/-}$, *and lal*$^{+/-}$) breeding stock on a pure BALB/c (*npc1* and *npc2*) or FVB/N background (*lal*) (17–20). In one group of experiments, *npc1*$^{-/-}$/*npc2*$^{-/-}$ mice were generated from heterozygous *npc1*$^{+/-}$/*npc2*$^{+/-}$ breeding pairs, and their litter mates (*npc1*$^{+/+}$/*npc2*$^{+/+}$) served as controls. From a total of 429 offspring, eight *npc1*$^{-/-}$/*npc2*$^{-/-}$ pups were obtained (1.9% of the total). This compares favorably with the frequency of 2.8% reported by Sleat et al. (17). Pups were genotyped at 19 days of age, except in those experiments using 7-day-old animals, where the pups were genotyped at 5 days of age (3, 17–20). Animals were group-housed in plastic colony cages in rooms with alternating 12 h periods of dark and light and were studied in the fed state at the end of the dark phase. There were comparable numbers of males and females in each group (21). All experimental protocols were approved by the Institutional Animal Care and Use Committee of The University of Texas Southwestern Medical School.

Diets and treatments

Animals were fed ad libitum a cereal-based, low-cholesterol (0.02% cholesterol, 4% total fat, w/w) diet (no. 7001; Harland Teklad, Madison, WI) upon weaning. Groups of mice were administered a subcutaneous injection at the scruff of the neck of a 20% (w/v, in isotonic saline) solution of either 2-hydroxypropyl-β-cyclodextrin (Sigma;productH107) (HP-β-CD), 2-hydroxypropyl-α-cyclodextrin (Aldrich; product 390690) (HP-α-CD) or sulfobutyl ether-7-β-cyclodextrin (CyDex Pharmaceuticals, Inc.) (SBE7-β-CD) [4,000 mg/kg body weight (bw)], during the late dark phase (21). Matching mice injected with saline alone served as controls. In one set of experiments, *npc1*$^{-/-}$ and *npc2*$^{-/-}$ mice were injected with variable doses of HP-β-CD at 49 days of age and studied 24 h later.

Tissue cholesterol concentration, synthesis rates, and esters

Groups of mice were studied 24 h after the injection of either HP-β-CD, HP-α-CD, or SBE7-β-CD at 7 days of age. They were exsanguinated and the liver, spleen, lung, brain, and carcass were collected. Another group of mice was injected at 49 days of age and studied 24 h later. For these mice, the brain, liver, spleen, lung, small intestine, colon, stomach, kidneys, adrenals, gonads, and carcass were collected. These tissues were saponified in alcoholic potassium hydroxide and the cholesterol was extracted and quantitated by gas chromatography (14). Tissue total sterol contents (TC) are expressed as mg of cholesterol per whole organ (mg/organ). The cholesterol values found in every organ and in the remaining carcass were summed to give whole animal cholesterol pools, and these values are expressed as mg of cholesterol per kg bw

(mg/kg). Liver triacylglycerol contents were measured as described (22). Rates of cholesterol synthesis in all of the tissues were measured in vivo as previously described (8). These rates are expressed as the amount of [^{3}H]water incorporated into sterols per hour per organ (nmol/h/organ). The [^{3}H]water incorporation rates in all organs were summed and used to calculate the whole animal synthesis rates. These values were then converted to the absolute mg of cholesterol synthesized each day per kg bw (mg/day/kg) (8). Esterified cholesterol levels in tissues were measured as described (23) and are expressed as mg of cholesterol in cholesteryl esters per organ (mg/organ). Plasma TC concentrations were measured by gas chromatography and expressed as mg/dl.

Determination of relative mRNA levels

RNA was obtained from mouse tissue using RNA STAT60 (Tel-Test, Inc., Friendswood, TX). For Northern analysis, mRNA was isolated using oligo(dT)-cellulose columns (Pharmacia Biotech). The isolated mRNA was prepared by pooling equal quantities of total RNA from 3–10 male mice per tissue (except for ovary, placenta, and uterus); 5 μg/lane was size-fractionated on 1% formaldehyde agarose gels and transferred to Zetaprobe nylon membranes (Bio-Rad Laboratories, Hercules, CA). The cDNA fragments of mouse NPC1 (nucleotides 1605–2629, NM_008720) and NPC2 (nucleotides 319-1253, NM_023409), and rat cyclophilin cDNA (kindly provided by David Russell, University of Texas Southwestern Medical Center) were ^{32}P-labeled using the Rediprime II Random Prime labeling system. The Northern blot membranes were hybridized with the radiolabeled probes, washed, and exposed to film. Quantitative real-time PCR was performed using an Applied Biosystems 7900HT sequence detection system and SYBR-green chemistry as previously described (8, 24). The mRNA levels are expressed relative to the housekeeping gene, cyclophilin, calculated by the comparative C_T method (25), and mathematically adjusted to set the control group in each experiment as a unit of 1.0.

Liver function tests

Plasma alanine aminotransferase (ALT) and aspartate amino transferase (AST) activities were determined by a commercial laboratory.

ED_{50} values for HP-β-CD

Cholesterol synthesis was measured in multiple organs in 49-day-old *npc1*$^{-/-}$ and *npc2*$^{-/-}$ mice after administration of varying doses of HP-β-CD to determine the ED_{50} in each organ. The doses of HP-β-CD administered were 0, 40, 100, 200, 300, 400, 500, 700, 1,000, 2,000, 4,000, and 8,000 mg/kg whole animal body weight. All mice were studied 24 h later.

Survival studies

The general condition of the mice was monitored daily. Once the animals began to show difficulty accessing the pelleted diet, they were provided a powdered form of the diet. When the mice were no longer able to take in food or water, they were euthanized, and this was considered the day of death.

Data analysis

All data are presented as a mean ± 1 SEM. Differences between means in groups were tested for significance ($P < 0.05$) using one-way ANOVA followed by the Newman-Keuls multiple comparison test (GraphPad Software, Inc., San Diego, CA). Differences between groups that are significant are designated with different letters. To establish the ED_{50} values, individual data points (n = 68 for *npc1*$^{-/-}$, n = 53 for *npc2*$^{-/-}$) were fitted to sigmoid curves and analyzed using the log (inhibitor) versus response equation to determine the $\log_{10}$ concentration that provokes a response equal to 50% (GraphPad Software, Inc.).

RESULTS

Alterations in cholesterol metabolism in *npc2*$^{-/-}$, *npc1*$^{-/-}$, and *lal*$^{-/-}$ mice

Initial experiments addressed the question of whether the lysosomal export defect was quantitatively similar in mice lacking any one of the proteins involved in sterol metabolism in the late E/L compartment. Although such data are partially available for the *npc1*$^{-/-}$ mouse (8, 14, 19), there are no similar published data for the *npc2*$^{-/-}$ or the *lal*$^{-/-}$ animals. As shown in **Fig. 1**, virtually every tissue in the mature *npc*$^{+/+}$ mouse expressed mRNA for both NPC1 and NPC2 to varying degrees, although there was poor correlation between the relative level of expression and the known rates of UC flux across each of these organs. These findings are consistent with the view that all organs must deal with the uptake of at least small amounts of plasma sterols.

The first studies utilized 49-day-old *npc2*$^{-/-}$, *npc1*$^{-/-}$, and *lal*$^{-/-}$ animals along with appropriate *npc2*$^{+/+}$, *npc1*$^{+/+}$, and *lal*$^{+/+}$ controls. Whereas both the *npc1*$^{-/-}$ and *npc2*$^{-/-}$ groups had normal brain size (**Fig. 2A**), both had significant hepatomegaly (Fig. 2B) and relative enlargement of the spleen (Fig. 2C) but not of most other organs (Fig 2E, F). Absolute body weights were reduced in both the *npc2*$^{-/-}$ and *npc1*$^{-/-}$ animals (Fig. 2G). The content of TC in brain, which takes into account both TC concentration (mg/g) and organ weight (g), was equally reduced in both types of mutant animals (Fig. 2H) because of neurodegeneration and demyelination. However, this parameter was significantly elevated in most other organs. The TC content in the liver, for example, reached 31 and 26 mg/organ, respectively, in the *npc1*$^{-/-}$ and *npc2*$^{-/-}$ mice, as opposed to only 2.9 mg/organ in control animals (Fig. 2I). Similarly, in most other organs the cholesterol content was elevated in the mutant mice, but this elevation was quantitatively less in the *npc2*$^{-/-}$ animals (Fig. 2J–M). Of importance, in this latter group, the level of CE in the liver (0.5 mg/organ), spleen (0.02 mg/organ), and other

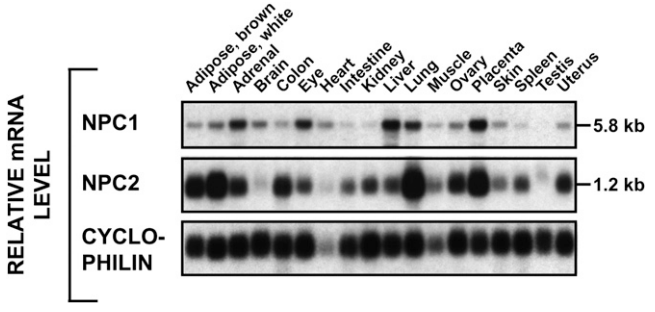

Fig. 1. Tissue distribution of NPC1 and NPC2 mRNA in normal mice. RNA was pooled from 3–10 mice for each organ (all males except for uterus, ovary, and placenta) and evaluated using Northern analysis.

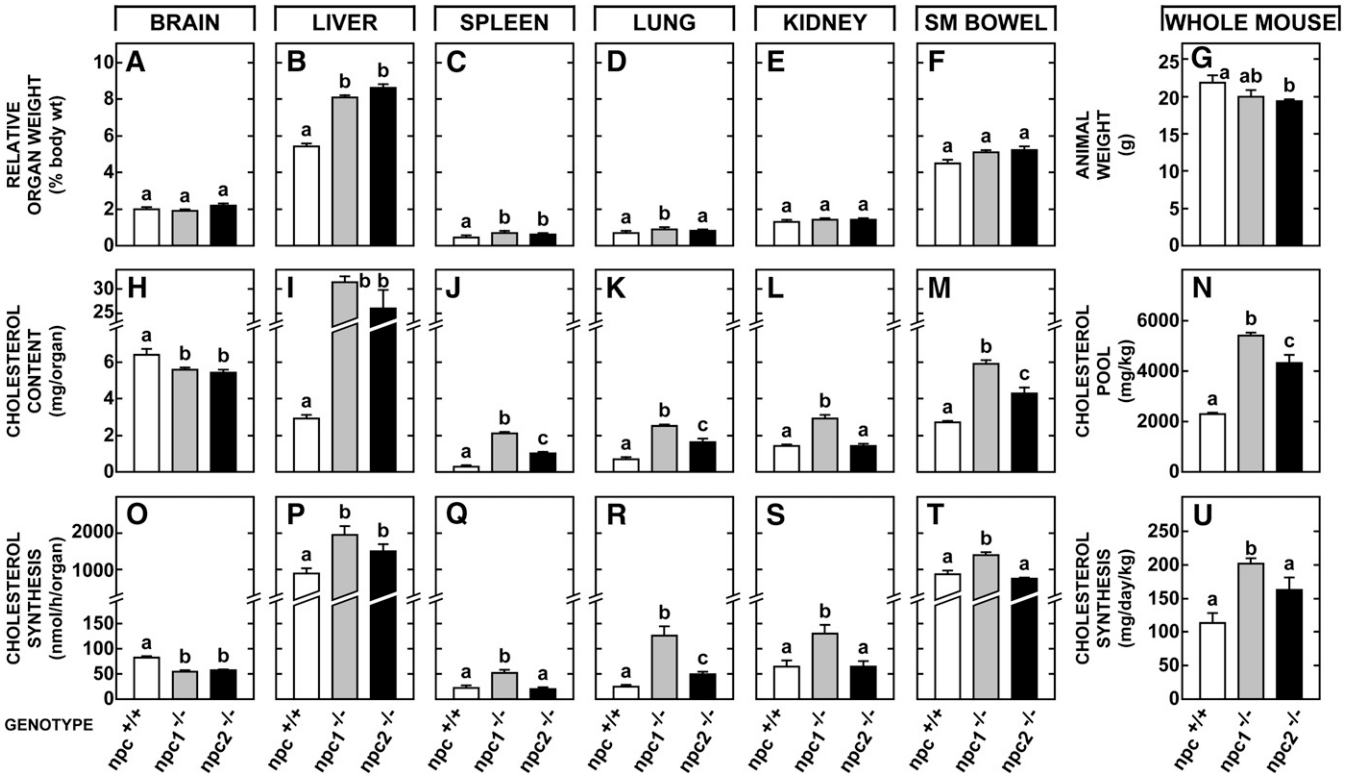

Fig. 2. Alterations in cholesterol metabolism in the *npc2*$^{-/-}$ mouse compared to those seen in the *npc1*$^{-/-}$ animal. Groups of *npc*$^{+/+}$, *npc1*$^{-/-}$, and *npc2*$^{-/-}$ animals were studied at 49 days of age. The *npc*$^{+/+}$ group included combined data derived from both *npc1*$^{+/+}$ and *npc2*$^{+/+}$ animals because these were virtually identical. Relative organ weight is expressed as a percentage of whole animal weight. Cholesterol content is given as the mg of cholesterol present in each whole organ and rates of sterol synthesis are also expressed per whole tissue. From these data, whole animal weights (G), cholesterol pools (N), and synthesis rates (U) were calculated. The columns represent means ± 1 SEM for 6–14 mice in each group, and significant differences ($P < 0.05$) among the groups are indicated by different letters.

tissues was very low so that, like the *npc1*$^{-/-}$ animals, the sequestered sterol in the *npc2*$^{-/-}$ mice was nearly all unesterified. When all tissues were combined, the whole animal TC pool increased from 2,305 mg/kg in the control mice to 5,408 mg/kg in the *npc1*$^{-/-}$ animals, but to only 4,337 mg/kg in the *npc2*$^{-/-}$ mice (Fig. 2N). In contrast, in 49-day-old *lal*$^{-/-}$ animals, this whole animal TC pool reached 9,480 ± 39 mg/kg and nearly all of this increase was as CE (not shown in Fig 2).

There was a small decrease in sterol synthesis in the brain (Fig. 2O) of the *npc2*$^{-/-}$ animals as described in *npc1*$^{-/-}$ mice (26). In contrast, rates of synthesis were elevated in most other organs, particularly in the *npc1*$^{-/-}$ animals. In liver, for example, sterol synthesis increased from 868 nmol/h/organ in *npc1*$^{+/+}$ mice to 1,958 and 1,501 nmol/h/organ, respectively, in the *npc1*$^{-/-}$ and *npc2*$^{-/-}$ animals (Fig. 2P). Similarly, in most of the other organs this compensatory increase in synthesis was less in the *npc2*$^{-/-}$ mice than in the *npc1*$^{-/-}$ animals (Fig. 2Q–T). As a result, the rate of UC synthesis in the whole animal increased from 113 mg/day/kg in the *npc*$^{+/+}$ mice to 163 mg/day/kg in the *npc2*$^{-/-}$ animals, but to 202 mg/day/kg in the *npc1*$^{-/-}$ mutants (Fig. 2U) and to 344 ± 11 mg/day/kg in the *lal*$^{-/-}$ animals (not shown in Fig. 2).

In three 49-day-old *npc1*$^{-/-}$/*npc2*$^{-/-}$ mice, the level of UC found in the liver (30.4 mg/organ), lung (3.5 mg/organ), kidney (2.3 mg/organ), and other organs was nearly identical to the values seen in the *npc1*$^{-/-}$ mice. Similarly, the compensatory increase in synthesis measured in the liver (2,355 nmol/h/organ), lung (149 nmol/h/organ), and other organs was about the same as in the animals lacking NPC1 function alone. These measurements yielded a whole animal TC pool of 5,498 mg/kg and a synthesis rate of 212 mg/day/kg. Thus, importantly, in the *npc1*$^{-/-}$/*npc2*$^{-/-}$ mice, where the sequestered sterol was all UC, loss of function of both proteins resulted in an export defect that essentially equaled that seen with loss of NPC1 function alone. Furthermore, this export defect was still significantly less severe than that seen in the *lal*$^{-/-}$ mice where the sequestered sterol was all CE.

Metabolic and clinical abnormalities in *npc2*$^{-/-}$ mice compared to those seen in *npc1*$^{-/-}$ animals

The next study explored whether the subtle differences in UC metabolism in these mice strains were also manifest in other measures of lipid metabolism and tissue damage. The *npc2*$^{-/-}$ mice had hypercholesterolemia (**Fig. 3A**) and reduced hepatic fatty acid synthesis (Fig. 3F) similar to that found in the *npc1*$^{-/-}$ animals. In the liver of *npc2*$^{-/-}$ mice, there was also a compensatory increase in the mRNA of NPC1 (Fig. 3B) just as the *npc1*$^{-/-}$ animals revealed an increased expression of NPC2 (Fig. 3C). Both mutant groups had nearly identical increases in mRNA levels for the inflammation markers CD68 and CD11c in the liver

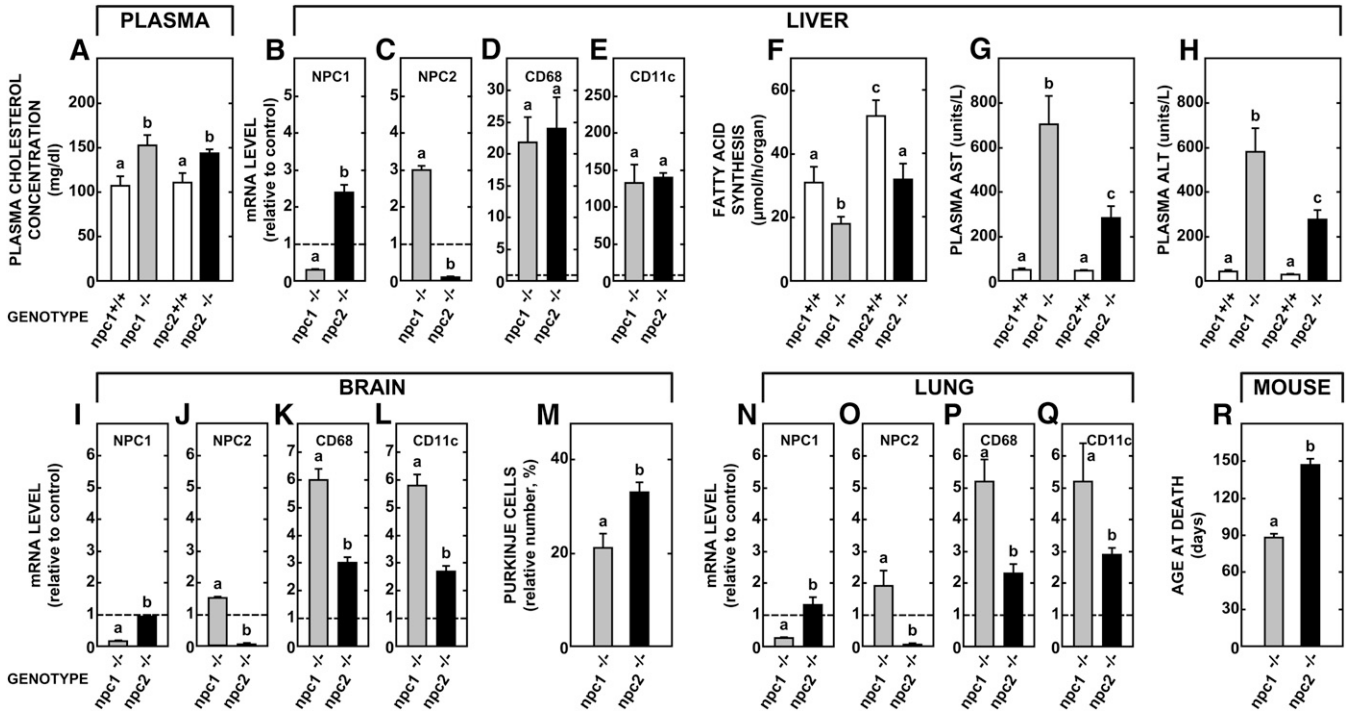

Fig. 3. Comparison of various molecular, metabolic, and clinical parameters in the $npc2^{-/-}$ and $npc1^{-/-}$ mice. Groups of $npc1^{+/+}$, $npc2^{+/+}$, $npc1^{-/-}$, and $npc2^{-/-}$ mice were studied at 49 days of age and a variety of measurements were made, both in vivo and in vitro. These include the relative expression of mRNA for several markers of inflammation, plasma lipid levels, and rates of hepatic fatty acid synthesis, and various clinical measures of hepatic and brain disease. The mRNA levels shown for the $npc1^{-/-}$ and $npc2^{-/-}$ mice are expressed relative to the appropriate $npc1^{+/+}$ and $npc2^{+/+}$ control animals (set at 1.0). The columns represent means ± 1 SEM of 6 (mRNA measurements) or 6–12 animals in each group. The survival studies (R) utilized 76 $npc1^{-/-}$ and 14 $npc2^{-/-}$ animals. Significant differences ($P < 0.05$) among groups are indicated by different letters.

(Fig. 3D, E). However, the level of hepatic damage, as reflected by the plasma AST and ALT levels, was significantly less in the $npc2^{-/-}$ animals (Fig. 3G, H). Brain did not show the same increases in mRNA levels for NPC1 and NPC2 (Fig. 3I, J), and the levels for CD68 and CD11c were less elevated in the $npc2^{-/-}$ mice (Fig. 3K, L). In addition, greater numbers of Purkinje cells survived at 49 days of age in the $npc2^{-/-}$ mice (Fig. 3M) although there was still significant neurodegeneration. Similar findings were seen in the lung. There was a blunted, compensatory response in NPC1 and NPC2 mRNA (Fig. 3N, O), and lower expression of CD68 and CD11c in the $npc2^{-/-}$ mice (Fig. 3P, Q). Given these observations, it was not surprising that the $npc2^{-/-}$ animals lived significantly longer (146 days) than the $npc1^{-/-}$ mutants (89 days) (Fig. 3R). Thus, the $npc2^{-/-}$ mice had a milder UC transport defect and a commensurately milder clinical picture.

Ability of the cyclodextrin, HP-β-CD, to bypass the function of either NPC2 or NPC1

These initial investigations identified important quantitative differences in the magnitude of the transport defect in the group of animals with inactivation of NPC2, NPC1, LAL, and, therefore, the level of sterol sequestration at 49 days of age. Although the $lal^{-/-}$ mice had accumulated sterol as CE at a rate of 148 mg/day/kg, the rates of accumulation of sterol as UC in the $npc1^{-/-}$ (63 mg/day/kg) and $npc2^{-/-}$ (41 mg/day/kg) mice were much lower. The next set of studies, therefore, explored whether more marked differences in the function of NPC1 and NPC2 could be identified based on the ability of HP-β-CD to reverse the transport defect in these two different groups of mutants. The most immediate and sensitive index of the increased flow of sterol into the cytosol following cyclodextrin administration is suppression of the rate of UC synthesis that is brought about largely by rapid ubiquitination and degradation of the key enzyme in the biosynthetic pathway, HMG CoA reductase (27). Taking advantage of this observation, $npc1^{-/-}$ and $npc2^{-/-}$ mice that were 49 days old were administered doses of HP-β-CD varying from 0 to 8,000 mg/kg and rates of UC synthesis in various organs were measured 24 h later. These data were fitted to sigmoid curves to yield the effective $\log_{10}$-dose of the cyclodextrin that resulted in 50% inhibition of synthesis (ED_{50}) in these different organs. In the liver of the $npc1^{-/-}$ mice, this value was 2.36 (equivalent to 229 mg/kg) (**Fig. 4A**). Similar values were found in spleen (Fig. 4B) and most other organs, presumably because cyclodextrin rapidly achieves a volume of distribution equal to the total extracellular water (28). Three organs had very different ED_{50} values, however. The value in the kidney (Fig. 4C) was nearly l log unit less, likely reflecting active endocytosis in the proximal tubule of molecules like cyclodextrin that are cleared through the glomeruli (29). In contrast, the ED_{50} in the brain (Fig. 4D) was over 2 log units higher than the liver, a finding indicative of the greater resistance

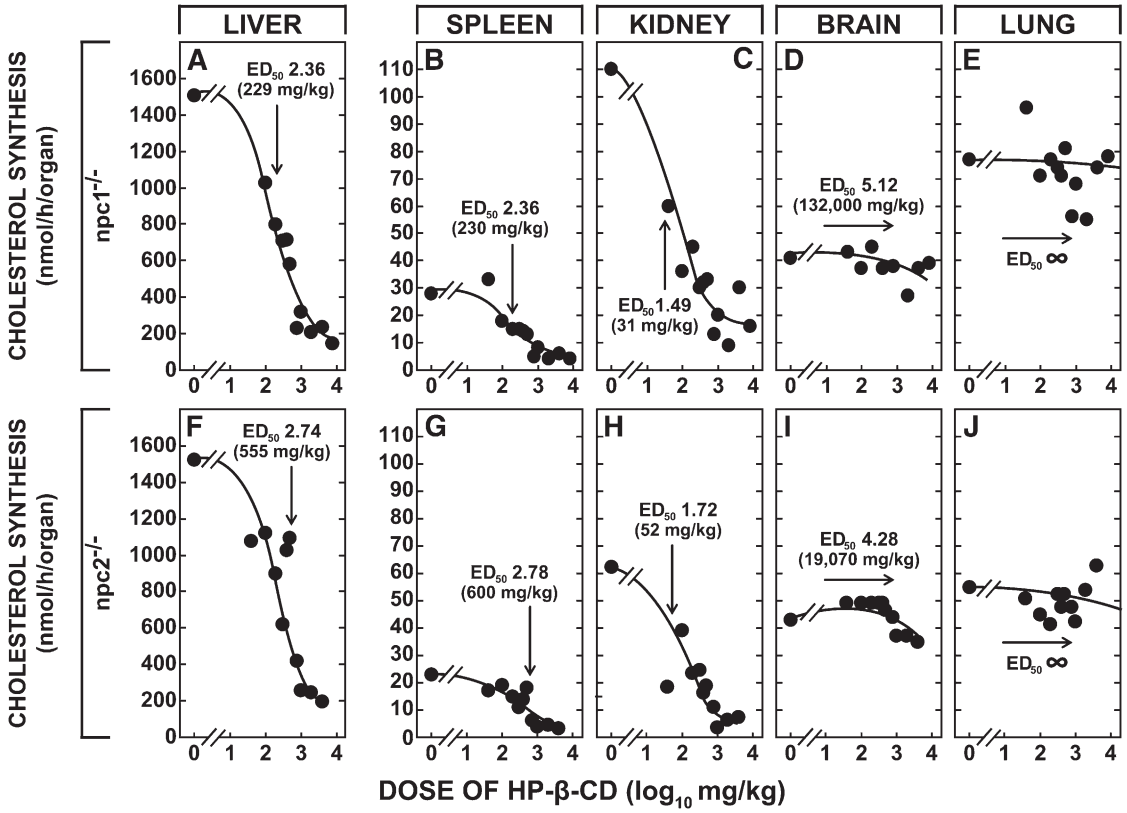

Fig. 4. The effective dose (ED_{50}) of HP-β-CD leading to 50% suppression of cholesterol synthesis in various organs of the *npc1*$^{-/-}$ and *npc2*$^{-/-}$ mice. Utilizing animals that were 49 days old, individual mice were given subcutaneously a dose of HP-β-CD that varied from 0 to 8,000 mg/kg. Twenty-four h later, the rate of cholesterol synthesis was measured in all of the major organs. The mean rates of synthesis at each dose are shown in this diagram. However, the sigmoid curves and ED_{50} values shown for each organ were generated by computer-fitting the individual data points from 68 *npc1*$^{-/-}$ and 53 *npc2*$^{-/-}$ animals (GraphPad Prism). These $\log_{10}$ ED_{50} values were also converted to the dose of HP-β-CD giving 50% inhibition of synthesis. In the case of the lung, the data points would not converge onto a sigmoid curve, i.e., the ED_{50} values were infinitely high.

to diffusion of this molecule across the capillaries of the CNS. Of particular interest, the lung (Fig. 4E) did not respond at all to administration of HP-β-CD.

The export defect in the *npc2*$^{-/-}$ animals responded to HP-β-CD in a virtually identical manner. The ED_{50} values in the liver and spleen were similar (Fig. 4F,G) whereas that in the kidney was 1 log unit less and that in the brain was >1 log unit higher (Fig. 4H,I). Again, synthesis in the lung was not affected by cyclodextrin (Fig. 4J). These effects of HP-β-CD were specific for UC synthesis because the rate of fatty acid synthesis in the liver was constant across all doses and averaged 25.6 ± 2.6 and 30.6 ± 1.7 μmol/h/organ, respectively, in the *npc1*$^{-/-}$and *npc2*$^{-/-}$ mice. Finally, when three *npc1*$^{-/-}$/*npc2*$^{-/-}$ mice were administered HP-β-CD at a single dose of 4,000 mg/kg, synthesis in the liver declined from 2,355 to 346 nmol/h/organ and in the kidney from 149 to 25 nmol/h/organ, whereas the lung remained unchanged at 176 versus 149 nmol/h/organ. Thus, HP-β-CD reversed the lysosomal export defect equally well in *npc1*$^{-/-}$ and *npc2*$^{-/-}$ mice and, importantly, this molecule could correct the defect even when both NPC1 and NPC2 were nonfunctional in the same animal. Apparently, HP-β-CD was working through a mechanism that was independent of the specific functions of NPC2 and NPC1.

Mechanism of action of cyclodextrin in reversing the lysosomal export defect

The last set of experiments explored the critical questions of whether this reversal actually required the cyclodextrin to interact directly with UC and whether this interaction took place in the bulk-water phase or at the membrane interface in the late E/L compartment. These assays were carried out in 7-day-old mice that are exquisitely sensitive to the effects of cyclodextrin. As anticipated, HP-β-CD, which can interact with UC both in the bulk-phase water and at an interface (11, 15), overcame the export defect in the organs of the *npc1*$^{-/-}$ animals (**Fig. 5A**, F, K). The liberated UC reached the metabolically active pool and suppressed synthesis in proportion to the size of the UC pool sequestered in the liver (~97%), spleen (~70%), and tissues of the carcass (~42%). In contrast to that in HP-β-CD, the hydrophobic pocket in HP-α-CD is too small (~0.2 nm^2) to admit the UC molecule and so HP-α-CD cannot interact with sterol either in bulk-phase water or at a membrane interface. When this cyclodextrin was tested, it was totally inactive. The UC remained sequestered in the late E/L compartment and there was no suppression of sterol synthesis in the liver, spleen, or carcass (Fig. 5B, G, L). An alternative way to test the hypothesis that cyclodextrin must interact with the sterol is to alter

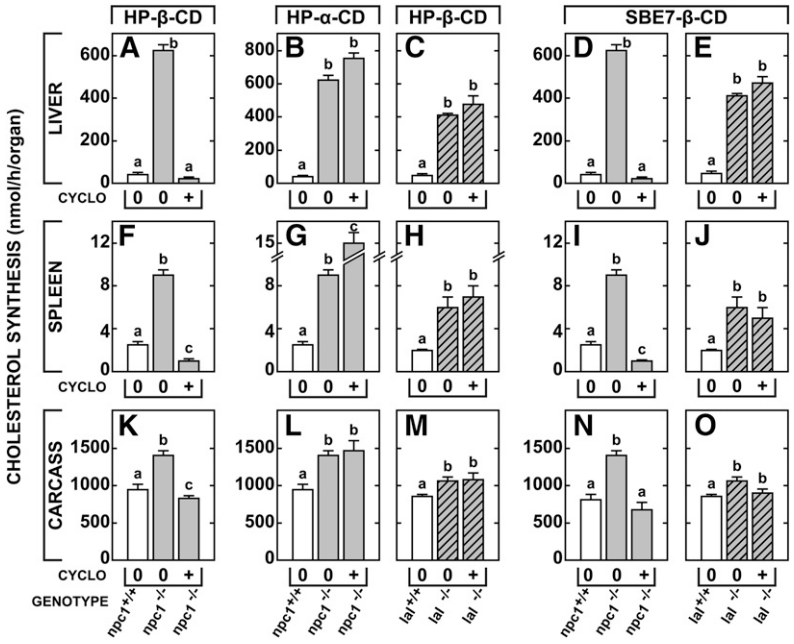

Fig. 5. The ability of HP-β-CD, HP-α-CD, and SBE7-β-CD to overcome the cholesterol export defect in $npc1^{-/-}$ and $lal^{-/-}$ mice. Seven-day-old mice of each genotype along with appropriate controls were administered a single subcutaneous dose of either HP-β-CD, HP-α-CD, or SBE7-β-CD (4,000 mg/kg). Twenty-four h later, rates of cholesterol synthesis were measured in various organs including the liver, spleen, and carcass. In this case, carcass refers to all residual tissues after removal of the liver, spleen, brain, and lungs, and consists mostly of muscle, bone, and adipose tissue. The columns represent means ± 1 SEM for 3–6 animals in each group and significant differences ($P < 0.05$) among groups are indicated by different letters.

the size and hydrophobicity of the substrate. The $lal^{-/-}$ mouse also accumulates cholesterol in the late E/L compartment, but in this case, the sterol is CE sequestered as a smectic liquid crystal (30). Because of their large size and the formidable free energy cost involved, CE molecules cannot move out of the crystal and interact with the cyclodextrin. As seen in Fig. 5C, H, M, when tested in the 7-day-old mouse model, even HP-β-CD had no effect in overcoming the processing defect found in the $lal^{-/-}$ mice.

The final, more subtle question to be explored was whether this interaction between the cyclodextrin molecule and UC took place in the bulk-phase water or at the membrane interface in the late E/L compartment. The HP-β-CD can form a 1:1 molecular complex with UC at a membrane interface or a 2:1 molecular complex that brings the sterol molecule into solution in the bulk-phase water. In contrast, the more highly charged sulfobutyl ether-7-β-cyclodextrin (SBE7-β-CD) can interact with UC at an interface, but cannot form a 2:1 molecular complex with UC and cannot solubilize the sterol molecule in bulk solution (31). Nevertheless, when tested in 7-day-old mice, SBE7-β-CD was just as effective as HP-β-CD in overcoming the transport defect in the $npc1^{-/-}$ animals (Fig. 5D, I, N), but again had no effect in the $lal^{-/-}$ animals (Fig. 5E, J, O). Taken together, these results are consistent with an earlier report that HP-β-CD exerted its effects in vivo without solubilizing UC and carrying the sterol to be excreted in the urine (14). Both HP-β-CD and SBE7-β-CD must be exerting their effects by interacting with UC at the interface between membranes in the late E/L compartment and the bulk-phase water within this compartment.

DISCUSSION

These studies provide the first quantitative comparison of the defects in lysosomal cholesterol processing that follow mutations inactivating LAL, NPC2, and NPC1, and give insights into how cyclodextrin may overcome these defects and prevent disease of the target organs. Virtually all cells express these three critical proteins, and all organs of the body are continuously taking up CE and/or UC associated with LDL, the remnants of VLDL and chylomicrons, and, in the CNS, apolipoprotein E (32, 33). In young adult mice, the magnitude of this sterol uptake throughout the body each day equals 120–140 mg per kg body weight. Not surprisingly, therefore, CE or UC accumulates in virtually every tissue of the $lal^{-/-}$, $npc2^{-/-}$, and $npc1^{-/-}$ animals (and children) (3, 19), and, in general, the severity of disease in a given organ is proportional to the amount of sterol sequestered in that organ (23, 34). However, the first important observation derived from the current studies is that the magnitude of the processing and export defect is very different, depending upon which protein is functionally absent. For example, by 7 weeks of age, the $lal^{-/-}$ mice had sequestered 7,241 mg of excess sterol per kg body weight (148 mg/day/kg), all as CE. In contrast, the amount of excess sterol accumulated in the $npc1^{-/-}$ mice was only 3,103 mg/kg (63 mg/day/kg) and was lower still in the $npc2^{-/-}$ animals (2,032 mg/kg, 41 mg/day/kg). In these latter two mutant groups, the sequestered sterol was all UC. These differences in rates of export were confirmed by the observed compensatory increases in UC synthesis in the cytosolic compartment of these same three mutant groups. The increase in synthesis was highest in the $lal^{-/-}$ mice (231 mg/day/kg) that had the most profound block in sterol movement from the E/L compartment into the cytosol. The increase in synthesis was significantly less in the $npc1^{-/-}$ (89 mg/day/kg) and $npc2^{-/-}$ (50 mg/day/kg) animals commensurate with the observation that significant amounts of sterol were still flowing from the late E/L compartment into the cytosol. Importantly, the rate of UC sequestration and the compensatory increase in synthesis found in $npc1^{-/-}/npc2^{-/-}$ mice were the same as in $npc1^{-/-}$

animals, a finding that suggests that these two proteins do act sequentially in moving UC from its site of generation by LAL to its site of exit from the E/L compartment, as suggested earlier. (17).

These marked differences in sterol sequestration in the *lal*$^{-/-}$ mice compared to the *npc1*$^{-/-}$ and *npc2*$^{-/-}$ animals very likely relate to the profound differences in physical behavior of the CE and UC molecules. When released from the lipoprotein, the very hydrophobic CE phases out of solution as smectic liquid crystals (30). Because of the formidable energy barrier, CE molecules cannot leave this crystal and interact with the phospholipid bilayers of the E/L membranes. In model systems, for example, the amount of CE that equilibrates with such membranes is <2 mol % (35). As a result, in the *lal*$^{-/-}$ mice, the CE is essentially irreversibly sequestered in the late E/L compartment of cells.

In contrast, when UC accumulates in this compartment, it presumably readily interacts with lipids of the bilayers (up to 50 mol % in model systems). This enrichment of the membranes with UC, in turn, may lead to secondary hydrophobic bonding with, and accumulation of, other amphipaths such as sphingolipids and bis(monoacylglycerol) phosphate with proliferation of multivesicular membrane structures within the E/L compartment (36). Although the "flip-flop" of UC across the bilayer may be somewhat restricted, diffusion along the plane of the leaflet is extremely rapid. In model membrane systems, diffusion coefficients of $\sim 10^{-8}$cm^2/sec are achieved (37). Thus, it is possible that this mobility accounts for the significantly lower rate of sterol sequestration in the *npc1*$^{-/-}$ and *npc2*$^{-/-}$ mice compared to the *lal*$^{-/-}$ animals because a portion of the UC may be able to move through these membranous structures independent of NPC1 and NPC2 to the exit site. This profound difference in behavior is seen even in whole animal or human experiments. When radio-labeled CE in a lipoprotein is administered to an animal, it remains sequestered in the particle until the ester is hydrolyzed; in contrast, when radio-labeled UC is similarly injected, it rapidly moves from the vascular space to multiple miscible pools throughout the body (38).

A more subtle question raised by these studies is whether the transport defect is slightly less severe in the *npc2*$^{-/-}$ mice compared to that seen in the *npc1*$^{-/-}$ animals. One explanation for this difference may be that the *npc2*$^{-/-}$ mice used in these studies are reported to be severe hypomorphs that have ~4% of the normal level of NPC2 expressed in the testes and epididymis (17). However, there apparently is no detectable NPC2 in the major organs of the body that determine net UC turnover rates, so it is unlikely that the higher rate of cholesterol movement out of the E/L compartment (~100 mg/day/kg) in the *npc2*$^{-/-}$ mice can be attributed to very small residual levels of NPC2 protein. Alternatively, this finding may imply that the function of NPC2 in initially binding UC is less critical than the role of NPC1 in moving the sterol to the exit site. Regardless, the findings in these animals further support the concept that the level of organ disease in these animals is directly related to the magnitude of UC sequestration.

Finally, these studies also provide new information on how the cyclodextrins are working to promote UC movement out of the late E/L compartment of cells into the cytosol where it is rapidly metabolized, transported to the liver, and, ultimately, excreted from the body as fecal acidic sterols (14). The observation that SBE7-β-CD can promote this rapid export of UC from the E/L compartment (Fig. 5) is consistent with the view that both HP-β-CD and SBE7-β-CD are interacting with UC at the membrane/bulk-water interface and not by solubilizing the sterol into the bulk-phase water of the E/L compartment. Presumably, this interaction facilitates the movement of UC through the complex membraneous structures in this compartment, as has been demonstrated in model membrane systems (39), elevating the export rate to values >200 mg/day/kg (8). Importantly, when one of the active cyclodextrins is present, apparently neither the function of NPC2 or NPC1 (or both) is required to maintain these high rates of UC movement out of the late E/L compartment into the cytosol.

Based on these new observations, it is possible to speculate on the nature of the biochemical and biophysical changes that occur in CE and UC metabolism following mutations of LAL, NPC2, and NPC1. As illustrated in **Fig. 6A**, cells throughout the body of normal animals acquire CE and UC from the receptor-mediated and bulk-phase uptake of a variety of lipoproteins. The sterol esters are hydrolyzed by LAL and the released UC is sequentially transferred to NPC2 and NPC1 before being exported from the lysosome, as has recently been delineated by in vitro binding studies (40, 41). It should be noted that the nature of the transport step leading to exit of UC from the lysosome has not yet been elucidated. This process, presumably, could be carried out by a transmembrane portion of NPC1 itself or by another as yet unidentified protein. Nevertheless, this series of events is so efficient that the rate of UC export from the E/L compartment of the mouse equals ~140 mg/day/kg (and much greater following cholesterol loading) and, as a consequence, the steady-state level of UC in the lysosomal membranes remains very low (42).

Inactivation of LAL totally disrupts this sequence of events, as illustrated in Fig. 6B. Once released from the lipoprotein, the very hydrophobic CE phases out of solution as smectic liquid crystals that can be readily identified by their birefringence in tissues from patients with Wolman disease (30). This CE is incapable of interacting with lipids of the lysosomal bilayer and so is essentially irreversibly trapped. Movement of cholesterol through the E/L compartment drops nearly to zero, and the tissues of the mouse accumulate ~140 mg/kg of sterol as CE each day. Cholesterol balance across each organ, and across the whole animal, is maintained, however, by an appropriate, massive increase in the rate of UC synthesis in the cytosolic compartment of cells throughout the body. The situation is very different, however, with mutations of NPC2 and NPC1, as illustrated in Fig. 6C. In these cases, CE is processed normally to UC and a portion of these molecules may phase out as crystals of cholesteryl monohydrate (43).

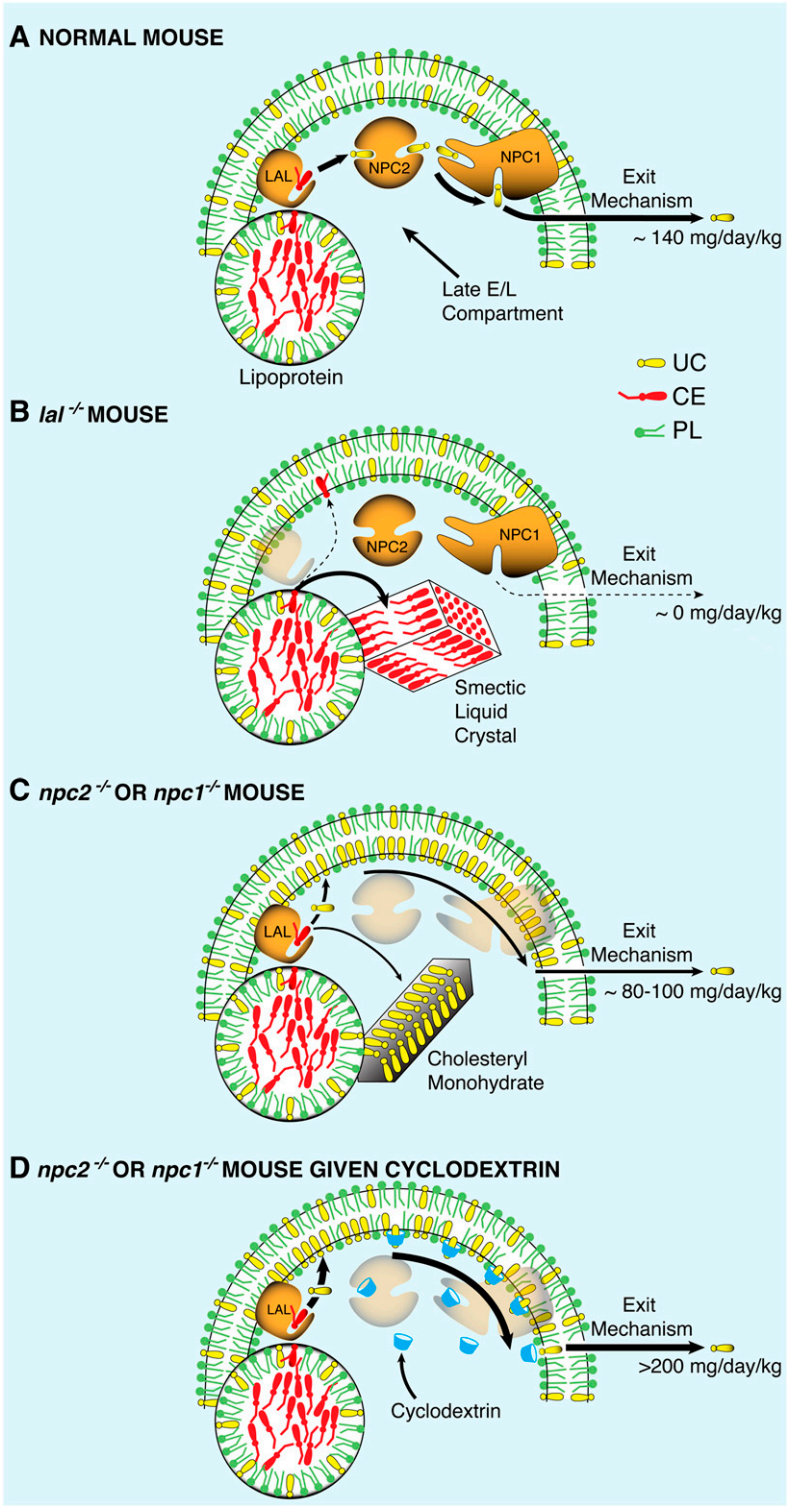

Fig. 6. Model illustrating cholesterol movement out of the late E/L compartment of cells into the cytosolic compartment. Lipoproteins carrying sterol esters enter the late E/L compartment where the CE normally is hydrolyzed by LAL, and the resulting UC is moved to the export site by the sequential activities of NPC2 and NPC1. In the normal adult mouse (A), the rate of UC movement through this pathway in all organs totals about 140 mg/day/kg. When LAL is nonfunctional (B), the CE is probably trapped in smectic liquid crystals, and UC output from the E/L compartment drops to near zero. However, when either NPC2 or NPC1 is mutated (C), UC continues to be generated and both interacts with the membrane phospholipids and precipitates as crystals of cholesteryl monohydrate. The UC in the wall of the lysosome presumably can still diffuse along the plane of the inner leaflet to the exit site so that, under these conditions, the rate of sterol movement out of the E/L compartment is only modestly reduced to 80–100 mg/day/kg. When cyclodextrin is administered to such animals (D), this rate of diffusion may be markedly increased.

More importantly, however, unlike CE, UC readily interacts with the lipids of the membranous structures of the E/L compartment and, presumably, can readily diffuse through these membranes to the site of exit from the lysosome. This situation likely explains why the export defect is relatively mild in NPC disease. The movement of UC through the late E/L compartment is only reduced from 140 mg/day/kg to 80–100 mg/day/kg in the *npc2*$^{-/-}$ and *npc1*$^{-/-}$ animals.

These studies also suggest that cyclodextrin may overcome the export defect in the *npc2*$^{-/-}$ and *npc1*$^{-/-}$ mice by facilitating this diffusion process (39). After administration, these hydrophilic oligosaccharides are rapidly distributed into the total extracellular water volume and circulate through the E/L compartment of cells by bulk-phase endocytosis (at rates of ~10–20 μl/h/g) (2). Not only does this cyclodextrin not solubilize UC into bulk-phase water when excreted in urine (14), but it also probably

does not solubilize UC within the E/L compartment of cells because SBE7-β-CD is just as effective as HP-β-CD in promoting cholesterol egress from the lysosome. Thus, as illustrated in Fig. 6D, these cyclodextrin molecules likely interact with UC at the bulk-phase water/lysosomal membrane interface to promote shuttling of the sterol molecules to the exit site.

In summary, these studies lend further credence to the concept that the magnitude of cell death and organ dysfunction in NPC disease is directly related to the amount of UC that accumulates in a particular group of cells and, further, that this disease can be prevented by measures that facilitate lysosomal UC clearance when either NPC2 or NPC1 is mutated. Unfortunately, one of the major target organs of NPC disease is the brain where there is widespread sequestration of UC in neurons and progressive neurodegeneration. Although systemic administration of HP-β-CD slows this neurodegeneration (9, 10), the very high ED_{50} values for the CNS (Fig. 4) point up that it is likely this cyclodextrin will have to be delivered directly into the pericellular bulk-water of the brain rather than given systemically. It remains to be seen, however, whether combined systemic and intrathecal administration of compounds like HP-β-CD will, in fact, prevent the major clinical manifestations of NPC disease.

The authors thank Mario Saucedo, Jennifer Burg, and Carolyn Crumpton for their excellent technical assistance and Anne marie Kelsey for expert preparation of the manuscript. The authors express their appreciation to Dr. Peter Pentchev for supplying the original *npc1*$^{+/-}$ breeding stock, Dr. Peter Lobel for the *npc2*$^{+/-}$ breeding stock, and Drs. Gregory Grabowski and Hong Du for the *lal*$^{+/-}$ breeding stock.

REFERENCES

1. Brown, M. S., and J. L. Goldstein. 1986. A receptor-mediated pathway for cholesterol homeostasis. *Science.* **232:** 34–47.
2. Liu, B., C. Xie, J. A. Richardson, S. D. Turley, and J. M. Dietschy. 2007. Receptor-mediated and bulk-phase endocytosis cause macrophage and cholesterol accumulation in Niemann-Pick C disease. *J. Lipid Res.* **48:** 1710–1723.
3. Du, H., M. Duanmu, D. Witte, and G. A. Grabowski. 1998. Targeted disruption of the mouse lysosomal acid lipase gene: long-term survival with massive cholesteryl ester and triglyceride storage. *Hum. Mol. Genet.* **7:** 1347–1354.
4. Naureckiene, S., D. E. Sleat, H. Lackland, A. Fensom, M. T. Vanier, R. Wattiaux, M. Jadot, and P. Lobel. 2000. Identification of HE1 as the second gene of Niemann-Pick C disease. *Science.* **290:** 2298–2301.
5. Carstea, E. D., J. A. Morris, K. G. Coleman, S. K. Loftus, D. Zhang, C. Cummings, J. Gu, M. A. Rosenfeld, W. J. Pavan, D. B. Krizman, et al. 1997. Niemann-Pick C1 disease gene: homology to mediators of cholesterol homeostasis. *Science.* **277:** 228–231.
6. Goldstein, J. L., R. A. DeBose-Boyd, and M. S. Brown. 2006. Protein sensors for membrane sterols. *Cell.* **124:** 35–46.
7. Chawla, A., J. J. Repa, R. M. Evans, and D. J. Mangelsdorf. 2001. Nuclear receptors and lipid physiology: opening the X-files. *Science.* **294:** 1866–1870.
8. Liu, B., S. D. Turley, D. K. Burns, A. M. Miller, J. J. Repa, and J. M. Dietschy. 2009. Reversal of defective lysosomal transport in NPC disease ameliorates liver dysfunction and neurodegeneration in the *npc1*$^{-/-}$ mouse. *Proc. Natl. Acad. Sci. USA.* **106:** 2377–2382.
9. Ramirez, C. M., B. L. Li, A. M. Taylor, J. J. Repa, D. K. Burns, A. G. Weinberg, S. D. Turley, and J. M. Dietschy. 2010. Weekly cyclodextrin administration normalizes cholesterol metabolism in nearly every organ of the Niemann-Pick type C1 mouse and markedly prolongs life. *Pediatr. Res.* **68:** 309–315.
10. Davidson, C. D., N. F. Ali, M. C. Micsenyi, G. Stephney, S. Renault, K. Dobrenis, D. S. Ory, M. T. Vanier, and S. U. Walkley. 2009. Chronic cyclodextrin treatment of murine Niemann-Pick C disease ameliorates neuronal cholesterol and glycosphingolipid storage and disease progression. *PLoS ONE.* **4:** e6951.
11. Thompson, D. O. 1997. Cyclodextrins - enabling excipients: their present and future use in pharmaceuticals. *Crit. Rev. Ther. Drug Carrier Syst.* **14:** 1–104.
12. Christian, A. E., M. P. Haynes, M. C. Phillips, and G. H. Rothblat. 1997. Use of cyclodextrins for manipulating cellular cholesterol content. *J. Lipid Res.* **38:** 2264–2272.
13. Small, D. M. 2003. Role of ABC transporters in secretion of cholesterol from liver into bile. *Proc. Natl. Acad. Sci. USA.* **100:** 4–6.
14. Liu, B., C. M. Ramirez, A. M. Miller, J. J. Repa, S. D. Turley, and J. M. Dietschy. 2010. Cyclodextrin overcomes the transport defect in nearly every organ of NPC1 mice leading to excretion of sequestered cholesterol as bile acid. *J. Lipid Res.* **51:** 933–944.
15. Okahata, Y., and Y. Xuanjing. 1989. Molecular selective assocations of cyclodextrins with lipid or cholesterol multibilayers cast on a piezoelectric crystal. *J. Chem. Soc. Chem. Commun.* 1147–1149.
16. Miyajima, K., H. Saito, and M. Nakagai. 1987. Interaction of cyclodextrins with lipid membrane. *J. Chem. Soc. Jpn.* **306:** 306–312.
17. Sleat, D. E., J. A. Wiseman, M. El-Banna, S. M. Price, L. Verot, M. M. Shen, G. S. Tint, M. T. Vanier, S. U. Walkley, and P. Lobel. 2004. Genetic evidence for nonredundant functional cooperativity between NPC1 and NPC2 in lipid transport. *Proc. Natl. Acad. Sci. USA.* **101:** 5886–5891.
18. Loftus, S. K., J. A. Morris, E. D. Carstea, J. Z. Gu, C. Cummings, A. Brown, J. Ellison, K. Ohno, M. A. Rosenfeld, D. A. Tagle, et al. 1997. Murine model of Niemann-Pick C disease: mutation in a cholesterol homeostasis gene. *Science.* **277:** 232–235.
19. Xie, C., S. D. Turley, P. G. Pentchev, and J. M. Dietschy. 1999. Cholesterol balance and metabolism in mice with loss of function of Niemann-Pick C protein. *Am. J. Physiol.* **276:** E336–E344.
20. Du, H., T. L. Cameron, S. J. Garger, G. P. Pogue, L. A. Hamm, E. White, K. M. Hanley, and G. A. Grabowski. 2008. Wolman disease/cholesteryl ester storage disease: efficacy of plant-produced human lysosomal acid lipase in mice. *J. Lipid Res.* **49:** 1646–1657.
21. Liu, B., H. Li, J. J. Repa, S. D. Turley, and J. M. Dietschy. 2008. Genetic variations and treatments that affect the lifespan of the NPC1 mouse. *J. Lipid Res.* **49:** 663–669.
22. Repa, J. J., S. D. Turley, G. Quan, and J. M. Dietschy. 2005. Delineation of molecular changes in intrahepatic cholesterol metabolism resulting from diminished cholesterol absorption. *J. Lipid Res.* **46:** 779–789.
23. Beltroy, E. P., B. Liu, J. M. Dietschy, and S. D. Turley. 2007. Lysosomal unesterified cholesterol content correlates with liver cell death in murine Niemann-Pick type C disease. *J. Lipid Res.* **48:** 869–881.
24. Valasek, M. A., and J. J. Repa. 2005. The power of real-time PCR. *Adv. Physiol. Educ.* **29:** 151–159.
25. Kurrasch, D. M., J. Huang, T. M. Wilkie, and J. J. Repa. 2004. Quantitative real-time polymerase chain reaction measurement of regulators of G-protein signaling mRNA levels in mouse tissues. *Methods Enzymol.* **389:** 3–15.
26. Xie, C., E. G. Lund, S. D. Turley, D. W. Russell, and J. M. Dietschy. 2003. Quantitation of two pathways for cholesterol excretion from the brain in normal mice and mice with neurodegeneration. *J. Lipid Res.* **44:** 1780–1789.
27. DeBose-Boyd, R. A. 2008. Feedback regulation of cholesterol synthesis: sterol-accelerated ubiquitination and degradation of HMG CoA reductase. *Cell Res.* **18:** 609–621.
28. Frijlink, H. W., J. Visser, N. R. Hefting, R. Oosting, D. K. Meijer, and C. F. Lerk. 1990. The pharmacokinetics of β-cyclodextrin and hydroxypropyl-β-cyclodextrin in the rat. *Pharm. Res.* **7:** 1248–1252.
29. Saito, A., H. Sato, N. Iino, and T. Takeda. 2010. Molecular mechanisms of receptor-mediated endocytosis in the renal proximal tubular epithelium. *J. Biomed. Biotechnol.* **2010:** 1–7.
30. Small, D. M. 1977. Liquid crystals in living and dying systems. *J. Colloid Interface Sci.* **58:** 581–602.
31. Rajewski, R. A., G. Traiger, J. Breshahan, P. Jaberaboansari, V. J. Stella, and D. O. Thompson. 1995. Preliminary safety evaluation of

parenterally administered sulfoalkyl ether beta-cyclodextrin derivatives. *J. Pharm. Sci.* **84:** 927–932.
32. Dietschy, J. M. 2009. Central nervous system: cholesterol turnover, brain development and neurodegeneration. *Biol. Chem.* **390:** 287–293.
33. Posse de Chaves, E. I., D. E. Vance, R. B. Campenot, R. S. Kiss, and J. E. Vance. 2000. Uptake of lipoproteins for axonal growth of sympathetic neurons. *J. Biol. Chem.* **275:** 19883–19890.
34. Repa, J. J., H. Li, T. C. Frank-Cannon, M. A. Valasek, S. D. Turley, M. G. Tansey, and J. M. Dietschy. 2007. Liver X receptor activation enhances cholesterol loss from the brain, decreases neuroinflammation, and increases survival of the NPC1 mouse. *J. Neurosci.* **27:** 14470–14480.
35. Hamilton, J. A., and D. M. Small. 1982. Solubilization and localization of cholesteryl oleate in egg phosphatidylcholine vesicles. *J. Biol. Chem.* **257:** 7318–7321.
36. Chevallier, J., Z. Chamoun, G. Jiang, G. Prestwich, N. Sakai, S. Matile, R. G. Parton, and J. Gruenberg. 2008. Lysobisphosphatidic acid controls endosomal cholesterol levels. *J. Biol. Chem.* **283:** 27871–27880.
37. Golan, D. E., M. R. Alecio, W. R. Veatch, and R. R. Rando. 1984. Lateral mobility of phospholipid and cholesterol in the human erythrocyte membrane: effects of protein-lipid interactions. *Biochemistry.* **23:** 332–339.
38. Goodman, D. S., R. P. Noble, and R. B. Dell. 1973. Three-pool model of the long-term turnover of plasma cholesterol in man. *J. Lipid Res.* **14:** 178–188.
39. Atger, V. M., M. de la Llera Moya, G. W. Stoudt, W. V. Rodrigueza, M. C. Phillips, and G. H. Rothblat. 1997. Cyclodextrins as catalysts for the removal of cholesterol from macrophage foam cells. *J. Clin. Invest.* **99:** 773–780.
40. Kwon, H. J., L. Abi-Mosleh, M. L. Wang, J. Deisenhofer, J. L. Goldstein, M. S. Brown, and R. E. Infante. 2009. Structure of N-terminal domain of NPC1 reveals distinct subdomains for binding and transfer of cholesterol. *Cell.* **137:** 1213–1224.
41. Abi-Mosleh, L., R. E. Infante, A. Radhakrishnan, J. L. Goldstein, and M. S. Brown. 2009. Cyclodextrin overcomes deficient lysosome-to-endoplasmic reticulum transport of cholesterol in Niemann-Pick type C cells. *Proc. Natl. Acad. Sci. USA.* **106:** 19316–19321.
42. Möbius, W., E. van Donselaar, Y. Ohno-Iwashita, Y. Shimada, H. F. G. Heijnen, J. W. Slot, and H. J. Geuze. 2003. Recycling compartments and the internal vesicles of multivesicular bodiesharbor most of the cholesterol found in the endocytic pathway. *Traffic.* **4:** 222–231.
43. Pentchev, P. G., E. J. Blanchette-Mackie, and E. A. Dawidowicz. 1994. The NP-C gene: a key to pathways of intracellular cholesterol transport. *Trends Cell Biol.* **4:** 365–369.